COMSOL® Analysis for Duct Acoustic

Mohamad. M. Ghulam[1], E. J. Gutmark[1]
1. Department of Aerospace Engineering, University of Cincinnati, Cincinnati, OH, USA

Abstract

The present work is a CAA analysis of an experiment was conducted at NASA Jet Propulsion Laboratory via using COMSOL® software. The experiment was investigating the driving mechanism of combustion instabilities in a small rectangular combustion duct. Two oscillatory acoustic modes were measured. The first one was around 285 cps that corresponded to the fundamental longitudinal mode of the duct. The second mode was the high-frequency oscillation around 3800 cps, which corresponded to roughly the fundamental antisymmetric transverse mode along the 4-in dimension of the duct. The latter mode was accompanied by driving mechanism that was vortex shedding from the lip of the flameholder. COSMOL® simulation analysis had very similar results with same shapes. The low-frequency was around 279 Hz and the high-frequency was around 3684 Hz. COMSOL results showed that both excited modes had half-wavelength pattern pressure waves, but in different directions (longitudinal and transverse). COMSOL validated that the frequencies were insensitive to flow rate, which has been shown in the experiment as well. COMSOL results included: 3D plots, and line graphs of the pressure acoustic field as well as the SPL of the excited modes. COMSOL analysis helped to understand the behavior of the modes inside the duct such as showing the locations of maximum and minimum amplitude of pressure waves (locations of maximum pressure amplitude where the acoustic modes tend to get excited). Therefore, COMSOL can help engineers and designers to build afterburner and combustion ducts with less severe thermo-acoustic instabilities. This can be done by suggesting proper locations of flameholder and fuel injectors inside the duct, so that heat release oscillations and pressure acoustic oscillations are out of phase. Eventually, a software application can be developed using COMSOL® Multiphysics for designing afterburners and combustion chambers.

Keywords: Thermo-acoustic instabilities, combustion, aeroacoustics, afterburners, duct acoustic, computational aeroacoustics, propulsion.

Introduction

Combustion or thermos-acoustic instability constitute a major problem in many fields of application from aerospace propulsion systems and gas turbine engines operating in the premixed mode to boilers and radiant heaters. These unsteady behaviors can lead to structural damaging, hardware melting, high noise, flame flashback or blowoff, enhanced heat transfer to liners, and overall systems failure. Combustion instability is still one of the highly active research areas, due to the need to understand the physical processes responsible of these instabilities. Considerable research and development efforts have been invested during the past half-century to elucidate the processes responsible for the excitation of these instabilities and the development of approaches to prevent them, especially for gas turbine combustors and afterburners.

On 1956 at NASA Jet Propulsion Laboratory, Roger and Marable conducted an experiment on combustion rectangular duct to investigate the mechanism drives thermosacoustic instabilities in ramjet combustors and afterburners, in particular the high frequency oscillation [ref.1]. The goal of the present work was to preform Computational Aeroacoustics "CAA" analysis via COMSOL® Multiphysics software to predict the frequencies, mode shapes, and behavior of the excited instabilities modes inside the duct, which were measured in the experiment.

Theories

A. Thermo-acoustic

Thermo-acoustic instabilities are spontaneously excited by a feedback loop shown in Figure 1 between oscillatory combustion processes and one of the natural acoustic modes of the combustor. Tim Lieuwen in his article [ref.2] explained that the two main factors responsible of these combustion instabilities are flame sensitivity to acoustic pressure perturbations and heat release rate oscillations. The first phenomena can be observed at home by placing speaker in front of a candle. The second phenomena occur because the combustion chamber is acoustically closed, so once sound is generated in the combustor, a little amount of sound waves escape. While, a great amount of sound waves "standing waves" are reflected from the upstream and downstream boundaries. Therefore, inherent fluctuations disturb the flame,

causing heat release oscillations. These heat release oscillations generate acoustic waves that propagate away from the flame, reflect off boundaries and re-imping upon the flame, which causes additional heat release oscillations. Therefore, the feedback loop is created (figure 1). However, in order for this to occur the heat release oscillation and pressure acoustic oscillation must be in phase. In other words, the heat release from combustion must be released when the acoustic pressure wave at or its maximum amplitude.

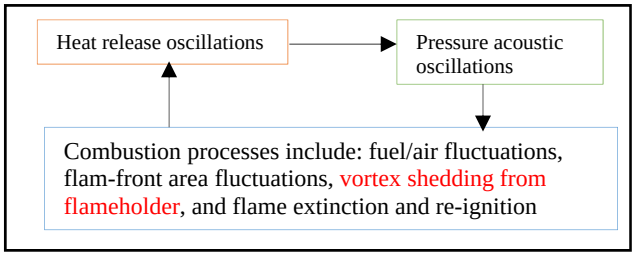

Figure 1. Basic feedback loop responsible for the instabilities.

Generally, thermo-acoustic instabilities are characterized by two distinct frequencies which are: low-frequency oscillation (rumble) and high-frequency oscillation (screech). The latter one was of particular interest in the experiment. The occurrence of these instabilities are mathematically expressed by Raleigh's criterion (eq.1). Rayleigh's criterion describes the condition under which unsteady heat release adds energy to the acoustic field [ref.3]. If the energy added (driving mechanism) by the combustion process to the acoustic modes exceeds the energy lost (damping mechanism), the energy of the mode will increase with time until it saturates at some limit-cycle.

$$\int_0^\tau \int_0^V p'(x,\, t)\, q' dv dt \geq \int_o^\tau \int_0^V \Phi(x,\, t)\, dv dt \quad \textbf{(eq.1)}$$

Where $p'$is acoustic pressure oscillation, $q'$is heat release oscillation, Φ is energy losses, τ is oscillation period, and V is duct volume.

B. Ducts' Standing waves & Boundary Conditions

There are two types of acoustic standing waves. First one is the longitudinal wave that travels in parallel with the direction of the fluid particles. The second type is the transverse wave which travels perpendicular to the fluid particles. To visualize these waves one can consider the motions of a fixed string as shown in Figure2. The most important factor for predicting the behavior of standing waves inside a duct is boundary condition. To study the pressure acoustics behavior inside a simple duct geometry, one can consider the standing sound wave patterns in a

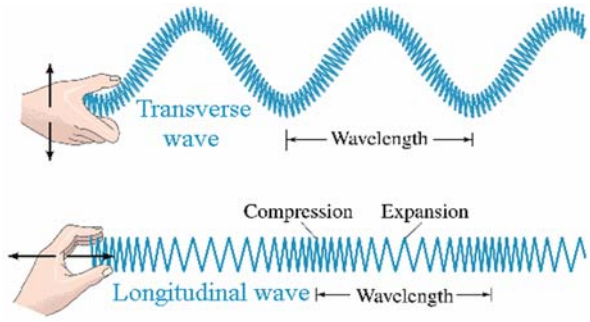

Figure 2. The transverse and longitudinal waves of a fixed string, which are similar to the acoustic standing waves inside a duct.

tube. The standing waves associated with resonance in a tube can be treated in terms of air displacement (velocity) and air pressure variations. Both have the same wave patterns, but completely in opposite directions. For instance, in an open boundary condition the pressure wave has a node and velocity wave has antinode (node: minimum frequency amplitude, antinode: maximum frequency amplitude). In a closed boundary the pressure wave has antinode while velocity wave has node. Figur3 shows the pressure standing waves with different boundary conditions.

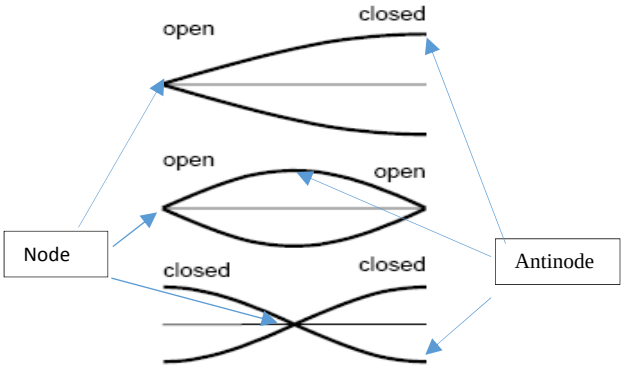

Figure 3. Pressure standing waves behavior for different boundaries.

C. Longitudinal Modes

1- Open-Open & Closed-Closed Boundary Conditions

The fundamental longitudinal mode of a duct with either two open-ended or close-ended boundaries is half-wavelength as illustrated in Figure 4. The mathematical expression for calculating the fundamental standing sound wave and any harmonic (overtones) waves is shown below:

$$f(any\ \#\ of\ harmonic) = \frac{any\ \#\ of\ harmonic * C}{2*L}$$ **(eq.2)**

where C is speed of sound, L is duct's length, and f is the frequency.

2- Open-Closed Boundary Condition

The combination of open and close boundaries results in a different reflected waves and therefore different standing wave patterns. The fundamental longitudinal mode has a quarter-wavelength pattern. The overtone harmonic waves and the fundamental one can be calculated using the following equation:

$$f(any\ \#\ of\ harmonic) = \frac{any\ \#\ of\ harmonic * C}{4*L}$$ **(eq.3)**

D. Transverse Modes

The previous equations (eq.2 and eq.3) are used to determine the harmonic longitudinal modes of a duct. In order to determine the acoustic transverse mode of the rectangular duct theoretically the "cut-on" frequency equation is used:

$$fm,n = \left(\frac{c}{2\pi}\right)\sqrt{(1-M^2)\{\left(\frac{m\pi}{H}\right)^2 + \left(\frac{n\pi}{W}\right)^2\}}$$ **(eq.4)**

Where H is height of the duct, W is width of the duct, M is the Mach number, and (m,n) represent modes of order. The values of the cut-on frequency equation represent the theoretical transverse acoustic modes that will propagate un-attenuated inside the rectangular duct. If an acoustic mode with a frequency below the cut-on frequency, it will be attenuated and exponentially decay with distance.

Experimental Combustion Duct and Conditions

The experiment was carried out in a small combustion duct of rectangular cross section in order that the observed phenomena would be of two-dimensional character. The combustion duct was of 1 inch by 4 inch and extended 24 ½ inch in length beyond the wedge-shaped flameholder. The apex of the flameholder was located 1 ½ inch away from the chamber inlet. The duct was fabricated of stainless steel. Mixtures of air and vaporized fuel entered a large plenum chamber to a converging nozzle having a contraction ration of 28/1, to the combustion duct, and then were discharged at atmospheric pressure. The experiment was conducted at atmospheric pressure level (1 atm), and the distributed average temperature inside the duct was 250 F. Figures 4 and 5 show the experimental combustion duct.

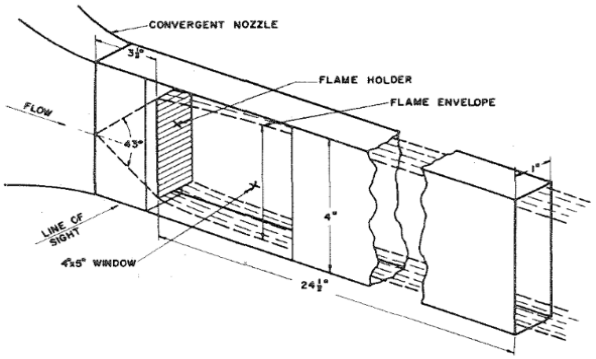

Figure 4. Schematic diagram of the experimental combustion duct.

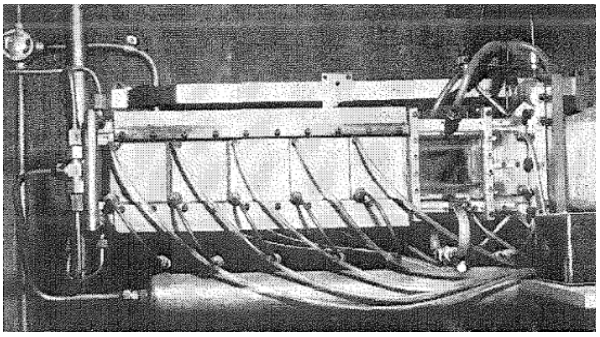

Figure 5. Side view of the actual combustion duct at NASA Jet Propulsion Laboratory.

Physics Interface & Simulation options

The Pressure Acoustic, Frequency Domain interface was used to perform the CAA analysis of the combustion duct. The physic interface solves the Helmholtz equation "homogenous wave equation" (eq.5) in the frequency domain for given frequencies, or as an eigenfrequency or model analysis study. This physics interface is suitable for modeling acoustics phenomena that do not involve fluid flow, which is the case here. Boundary conditions include sources, nonreflecting radiation conditions, impedance conditions, periodic conditions, far-field computation conditions, as well as interior boundary conditions such perforated plates.

$$\nabla * (-\frac{1}{\rho_c}(\nabla p_t - q_d) - \frac{k_{eq}^2\ p_t}{\rho_c} = Q_m$$ **(eq.5)**

$$p_t = p + p_b$$

$$k_{eq}^2 = \left(\frac{\omega}{c_c}\right)^2$$

$$\omega = 2\pi f$$

SYMBOL	QUANTITY	SI UNIT
$\rho_c = \rho$	density	$\left(\frac{kg}{m^3}\right)$
$C_c = C$	speed of sound	$\left(\frac{m}{s}\right)$
p	pressure	(Pa)
p_t	total pressure	(Pa)
p_b	background pressure	(Pa)
q_d	dipole domain source	$\left(\frac{N}{m^3}\right)$
Q_m	monopole domain source	$\left(\frac{1}{m^2}\right)$
ω	angular frequency	rad/s
k	wave number	$\left(\frac{1}{m}\right)$

Table 1. Symbols' definitions.

Generally, to predict the frequencies and mode shapes of the excited instabilities, we need to know the geometric characteristics of the duct, average temperature distribution, and boundary conditions. The first two were directly obtained from the experimental set-up. For determining the boundary conditions, equations 2 and 3 were used and compared later with the experimental values, their results are shown in table 2. The "acoustically" close-close boundaries assumption was the correct assumption for this experiment. Three factors support this assumption. The first one was that prior to the inlet there was a converging nozzle with contraction ratio of 28/1 as described previously. Second reason was that the duct's outlet was connected to an exhaust, which did not contribute to the acoustic field. Third one was that the fundamental longitudinal mode value computationally and mathematically for the close-close case were matching the experimental measured value, which will be illustrated in the next sections. Therefore, the sound hard boundaries were applied at the inlet and outlet. The ideal gas was selected for the fluid model. The fine tetrahedral mash was chosen for mesh analysis as shown in figure 6. The simulation did not account for flow.

Case 1	**Close-close**
Fundamental Longitudinal	279.817 Hz
Case 2	**Close-open**
Fundamental Longitudinal	139.909 Hz

Table 2. The calculated values for the fundamental longitudinal modes for different boundary conditions Equations 2 and 3 were used.

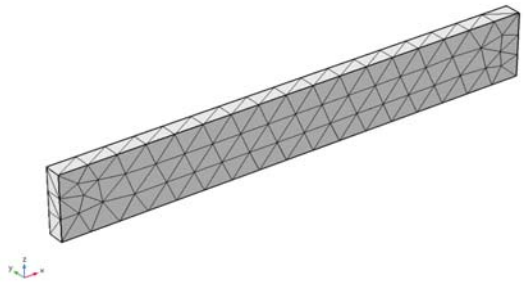

Figure 6. Fine free tetrahedral mesh.

Experimental Results

Two oscillatory modes were recorded during the experiment. The first one was the low-frequency oscillation that was about 280 cps and the high-frequency oscillation "screech" was about 3800 cps, Figure 7 illustrates the measured frequencies. The low-frequency oscillation corresponded to the fundamental longitudinal mode of the combustion duct as if it was closed at both ends, while the high-frequency oscillation corresponded roughly to the fundamental antisymmetric transverse mode across the 4-in dimension of the duct. The high-frequency component was of principal interest. Both instability modes have showed that they are unaffected by flow rate as shown in Figure 7. The frequency of screeching combustion oscillation is insensitive to changes in airflow rate through the combustion duct, only miner decrease was recorded at high Mach number. Figure 7 also shows that the fundamental longitudinal mode is completely unaffected by the changes in flow rate.

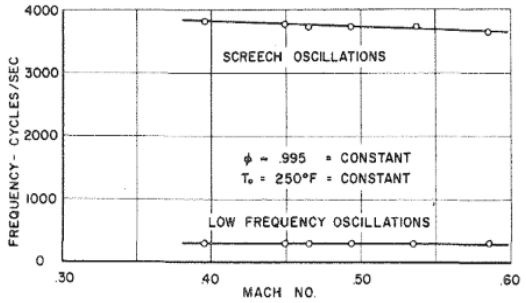

Figure 7. The frequencies of instability modes are not affected by flow rate.

A. The Driving Mechanism

The main goal of the experiment was to investigate the driving mechanism that excite the high-frequency oscillation "screech" mode of the combustion duct. The following mechanism of exciting the acoustic oscillation was suggested. The transverse velocity waves associated with the transverse acoustic pressure waves produce vortices at the lip of the flameholder

and moved them to the hot zone (area behind the flameholder). Figure 8 illustrates the formation of vortex induced by transverse velocity waves. These vortices contain of a large amount of combustible materials. When these combustible materials moved to the hot wake region by vortices, after an appropriate length of time they ignite and burn. The combustion of this large amount of material produce a pressure wave. If the generated pressure wave from the combustion process (heat release oscillation) is in phase with one of the natural acoustic mode of the duct, they are considered to be "coupled" and the excitation occur. In the present case the vortex shedding was off center in the duct, the antisymmetric mode of the duct was excited. Figure 9 shows a real image of the vortex shedding behind the flameholder accompanied the high-frequency screeching combustion.

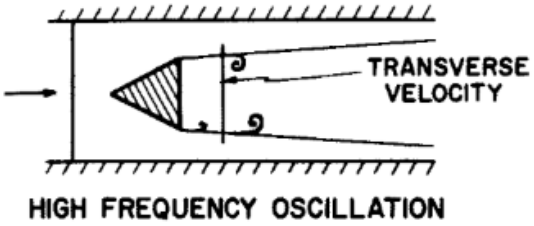

Figure 8. Vortices start to form at lip of flameholder due to transverse velocity waves.

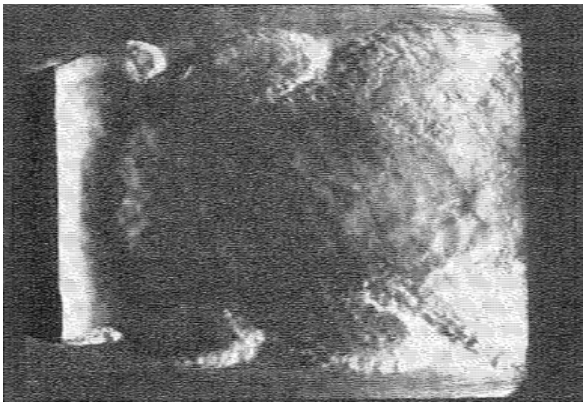

Figure 9. Photo of the vortex shedding accompanied with the high-frequency oscillations "screech" that was taken during the experiment.

COMSOL® Results

COMSOL simulation results include: 3D plot of the excited instability modes, and line graphs of the acoustic filed and sound pressure level (SPL). The low-frequency oscillation was found to be around 279.57 Hz and the high-frequency oscillation was found to be around 3684 Hz. It can be seen from Figure 10 that the low-frequency oscillation corresponded to the fundamental longitudinal (x-axis) mode with half-wavelength pattern, which matched the theoretical prediction (close-close case) and experimental measured value that were shown in table 2 and Figure 7 respectively. COMSOL simulation also found that the high-frequency oscillation corresponded to an antisymmetric transverse mode across the 4-in dimension (z-axis) of the duct as illustrated in Figure 11.

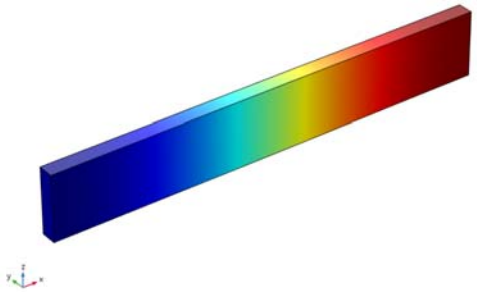

Figure 10. 3D plot of the acoustic pressure filed for the low-frequency oscillation, which was around 279.57 Hz (the fundamental longitudinal mode of the duct along the x-axis).

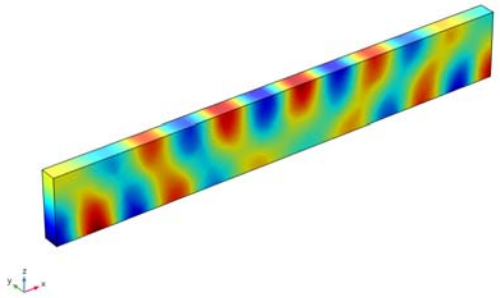

Figure 11. 3D plot of the acoustic pressure filed for the high-frequency oscillation, which is around 3684 Hz. (antisymmetric transverse mode along the z-axis)

In order to find the behavior of the instability modes along the duct, a line was drawn along the (x-axis) as shown in Figure 12. The line graphs of the acoustic pressure filed and SPL along the duct are shown in Figure 13. Another line was drawn 11-in away from the inlet and normal in the (z-axis) to the duct as shown in Figure 14. This line represents the pressure transducer that was located at this point for measuring the frequency oscillation in the experiment. This line was drawn to see the behavior of the antisymmetric transverse mode along the 4-in dimension of the duct. The corresponding results are illustrated in Figure 14 and 15. Similarly, a third line was drawn as shown in Figure 16 in the 1-in dimension (y-axis) of the duct for

predicting the behavior of the mods on that direction. The corresponding plots are illustrated in Figures 17 and 18.

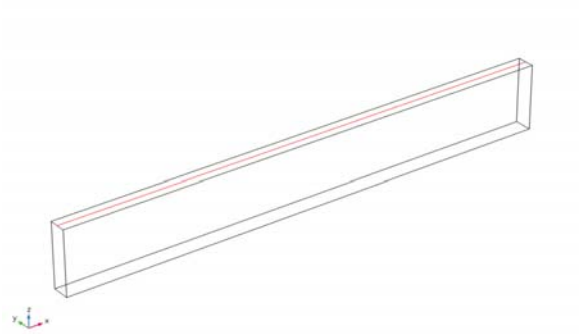

Figure 12. A line was draw along the x-axis to find the behavior of the mods in the longitudinal direction.

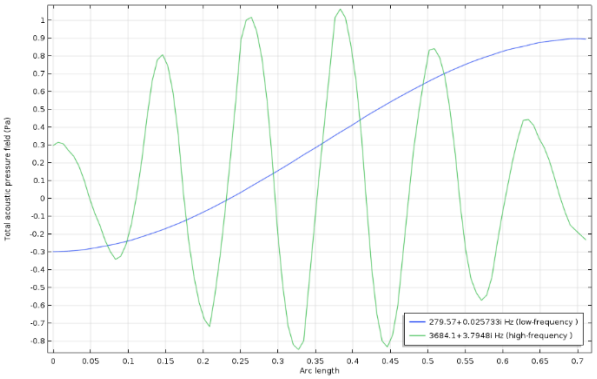

Figure 13. The acoustic pressure variations of the two modes along x-axis of the duct. (Blue line: low-frequency, green line: high-frequency).

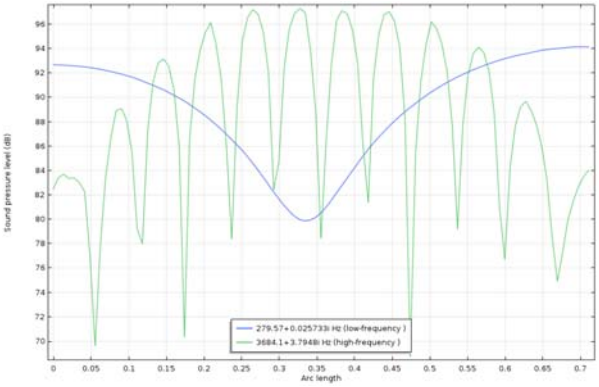

Figure 14. The SPL of the two modes along the duct (x-axis).

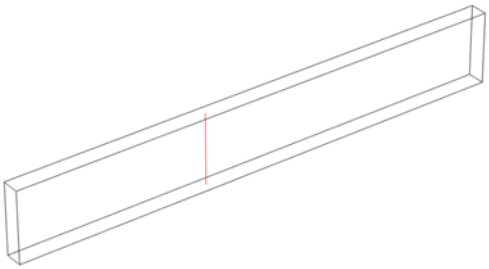

Figure 15. This line represents the pressure transducer, which was located normal to the surface in the z-axis and 11 in. away from the inlet.

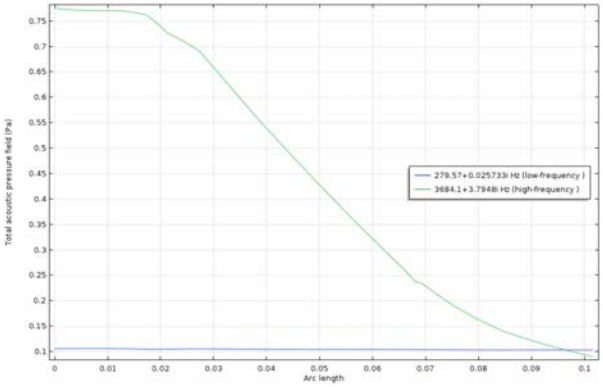

Figure 16. The acoustic pressure filed of the modes along the 4-in dimension of the duct (z-axis), where the pressure gage was located.

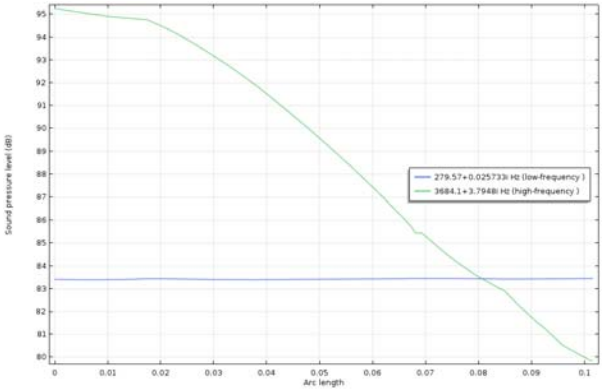

Figure 17. The SPL of modes along the z-axis. The SPL of the screech frequency is about 96 dB.

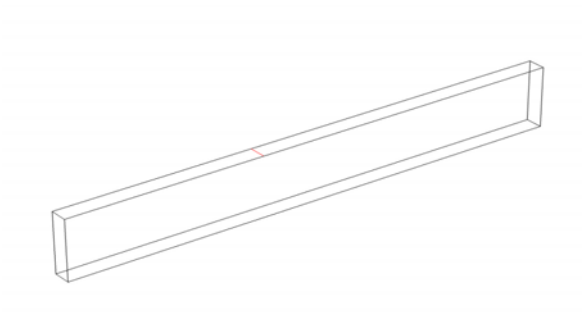

Figure 18.A third line was drawn along the y-axis to obtain more information about the behavior of the modes.

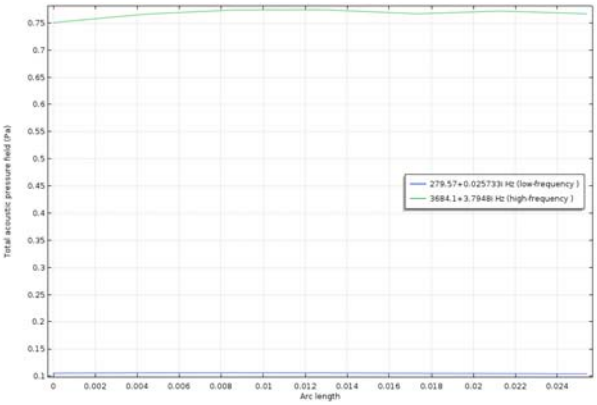

Figure 19. The acoustic pressure field of the modes along y-axis.

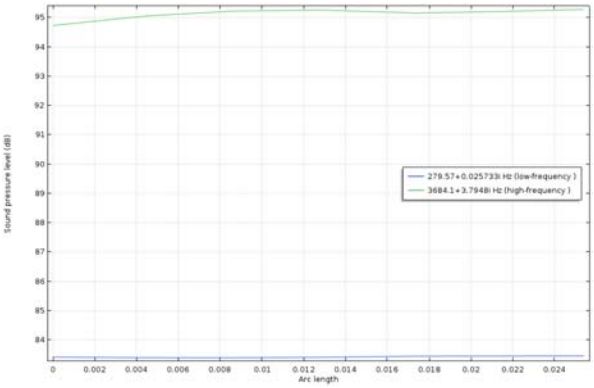

Figure 20. The SPL of the modes along y-axis.

Observations

COMSOL simulation results were in a great agreement with the measured values as shown in Table 3. COMSOL CAA analysis validated that the oscillation frequencies are not effected by flow, since the flow was not accounted during the simulation. Both experiment and simulation have shown that the low-frequency corresponded to the fundamental longitudinal mode of the duct, while the high-frequency oscillation corresponded to the fundamental antisymmetric transverse mode along the 4-in dimension of the duct. From COMSOL results in Figure 14 we can see that the high-frequency mode has a rapid changes in the longitudinal direction (x-axis), while the low-frequency mode has a half-wavelength pattern with antinodes at closed boundaries (inlet and outlet). Figure 16 shows the behavior of the modes along the 4-in dimension of the duct (z-axis), the high-frequency oscillation mode has also a half-wavelength pattern in the with antinodes at both sides, while the low-frequency mode has no interference and almost constant. Both modes are not remarkably changing along the 1-in dimension of the duct (y-axis) as illustrated in Figure 19.

As mention earlier the onset of the instability occur when the heat release oscillations from combustion are released where pressure acoustic modes near or at their maximum values (antinodes). Therefore, the estimated location for the low-frequency oscillation to get excited is at the inlet or outlet of the combustion duct. For the screeching frequency the excitation can occur in several locations at the central region of the duct.

	Low-frequency oscillation	High-frequency oscillation
Experimental results	285 cps	3800 cps
COMSOL results	279.57 Hz	3684 Hz

Table 3. The simulation results were in a great agreement with the experiment results

Concluding Remarks and Future Work

COMSOL CAA analysis demonstrated their usefulness on obtaining more information about the behavior of the excited instability modes inside the experimental combustion duct. The results included: 3D plots, and line graphs of the acoustic pressure filed as well as the SPL of the modes. One of the main advantages of using COMSOL was to estimate the location of instability excitation throughout the duct. COMSOL can be used to help designing afterburner ducts in aircraft. By analyzing the impacts of geometry, flameholder positions, and fuel injectors' location on the acoustic pressure field. This can be done by easily varying the geometry of the duct and find the most efficient shape. In addition, suggesting the proper locations for flameholder and fuel injectors inside the duct, so that heat release oscillations are not in phase with acoustic pressure waves at or near their maximum amplitude.

In the future, a software application can be developed via COMSOL® Multiphysics for designing combustion chamber and afterburner ducts. This app

will have great impact as it will to help engineers and designers build afterburner ducts with minimal acoustic instabilities and less experimental work. Therefore, it will save a great amount of time and reduce costs.

References

1. Don E. Rogers and Frank E. Marble, “A Mechanism for High-Frequency Oscillation in Ramjet Combustors and Afterburners”, The American Rocket Society, 1956.
2. Tim lieuwen, “Combustion Driven Oscillations in Gas Turbine”, Turbomachinery international, 2003.
3. Perry L. Blackshear, Warren D. Rayle, and Leonard K. Tower, “Study of Screeching Combustion in a 6-inch Simulated Afterburner”, National Advisory Committee for Aeronautics, 1955.
4. Oates, G. C., “Aerothermodynamics of Aircraft Engine Components”, American Institute of Aeronautics and Astronautics, New York, Ch. 2 Afterburners, 1985.
5. Houshang B. Ebrahimi, “Overview of Gas Turbine Augmentor Design, Operation and Combustion Oscillation”, American Institute of Aeronautics and Astronautics, 9-12 July 2006.
6. Guillaume Jourdain and Lars-Erik Eriksson, “Analysis of Thermo-acoustic Properties of Combustors and Afterburners”, Proceeding of ASME Turbo Expo, 2010.
7. Rienstra, sjoerd W, “Fundamental of Duct Acoustics”, 2015.
8. Cuppoletti, J.kastner, Reed Jr and E. J. Gutmark, “High frequency Combustion Instabilities with Radial V-Gutter Flameholders”, American Institute for Aeronautics and Astronautics , 2009.
9. Prateep Chatterjee, “A Computational Fluid Dynamics Investigation of Thermoacoustic Instabilities in Premixed Laminar and Turbulent Combustion Systems”, July 2004.
10. Ben T. Zinn and Timothy .C. Lieuwen, “Combustion Instabilities: Basic concepts”, Progress in Astronautics and Aeronautics, pages 3-26. American Institute of Aeronautics and Astronautics, 2005.
11. S. Sivasegaram, B. Thompson and J. Whitelaw, “Acoustic Characterization Relevant to Gas Turbine Augmentors”, American Institute for Aeronautics and Astronautics, 1989.
12. Hubbard, Harvey H, “Aeroacoustics of flight vehicles theory and practice”, the Acoustical Society of America, 1995.
13. Morfey, “Rotating pressure patterns in ducts: Their generation and transmission”, Journal of Sound and Vibration, 1964.
14. Morfey, “Sound Transmission and Generation in Ducts with Flow”, Journal of Sound and Vibration, 1971.
15. Jacobsen Finn, “Propagation of Sound Waves in Ducts”, Technical University of Denmark, 2000.